

The stability chart of parallel shear flows with double-diffusive processes – general properties

M. MAGEN, D. PNUELI and Y. ZVIRIN

Faculty of Mechanical Engineering, Technion, Israel Institute of Technology, Haifa, 32000, Israel

(Received September 12, 1984 and in revised form April 4, 1985)

Summary

The stability of an infinite fluid layer is considered, subject to horizontal flow and arbitrary initial vertical temperature and salinity distributions. Linear stability analysis is applied, using three-dimensional perturbations. A method is outlined for the construction of a general stability chart; parts of the chart are marginal-stability lines obtained by using the Squire theorem, where disturbances in the flow direction are the most unstable; necessary conditions for the theorem to be valid are developed. These conditions are shown to be sufficient in certain cases. A technique is presented to obtain the stability boundary even when these conditions are not satisfied. The results show that an increase in the Reynolds number cannot increase the stability domain.

1. Introduction

Flows with density gradients appear in many geophysical processes, in energy-conversion systems and in other engineering applications, where density variations are caused by temperature and concentration fields. The stability of such flows is often an important and even crucial problem, e.g., in atmospheric- or water-pollution control, where unstable situations may be favorable, leading to enhanced mixing and diffusion. The performance of the solar pond, on the other hand, depends on its stability and the continued maintenance of the stratification.

Rather extensive surveys of earlier work on the stability of fluids at rest subject to vertical temperature gradients only were presented by Ostrach [1] and Chandrasekhar [2].

Considerations of more than one stratifying agent appeared relatively later. Veronis [3] investigated stability of a fluid at rest with an adverse temperature gradient and a stabilizing salinity gradient. He found that the principle of exchange of stabilities does not hold in some cases, and neutral stability can occur with oscillations. Moreover, he also shows that instabilities of a fluid with these two gradients can occur even when the density decreases upwards.

Pnueli and Iscovici [4] obtained sufficient conditions for stability (either stationary or oscillatory) for a confined fluid with a temperature gradient and an arbitrary number of concentration gradients. A further survey of double-diffusive stability has been presented by Pnueli and Zvirin [5].

A rather small number of studies on stability of flows with initial distributions of temperature, salinity and velocity is available. Refs. [6–9] present studies of different flows with temperature gradients only.

Linden [10] investigated the stability of a shear flow in an infinite layer with linear temperature and salinity distributions. He concluded that for a two-dimensional perturbation system in the flow direction, a *state point* ([2], pp. 1–2) which is statically unstable, can become stable for a finite Reynolds number.

The present work is concerned with the stability of an infinite fluid layer with an arbitrary horizontal flow and arbitrary initial vertical temperature and salinity distributions. Plane waves of small disturbances are considered. These waves may be in the flow direction (transverse rolls), perpendicular to it (longitudinal rolls) or set at any angle. Koppel [6] suggested, based on the Squire theorem [11], that only transverse rolls need be used to check stability. Gage and Reid [7] have shown, however, that Koppel's conclusion does not always hold, because the Reynolds (Re) and Richardson (Ri) numbers are not invariant under the Squire transformation.

Other works, e.g. [7,8] obtained stability boundaries by using the Squire theorem, considering disturbances either in the flow direction or perpendicular to it. Linden [10] treated three-dimensional perturbations, but his work was restricted to small Reynolds numbers.

The present work shows that there exist flows which are stable for these disturbances but unstable for three-dimensional ones of neither direction. It outlines a method for deriving the general stability chart for arbitrary three-dimensional perturbations. Necessary conditions are also obtained for the use of the Squire theorem; these determine when two-dimensional disturbances are the most unstable, and correspond to the stability boundary. In some cases these conditions may also be sufficient. It is emphasized that the derivation is obtained from the eigenvalue equations, and not from their solution.

An additional result of this paper is that the stability domain can never increase by increasing the Reynolds number.

2. Governing equations

Consider a horizontal parallel flow of an incompressible fluid, perpendicular to the gravitational field \mathbf{g} , with vertical distributions of temperature and salt concentration. The Boussinesq approximation is used and a linear relation between temperature, salt concentration and density is assumed. The dissipation term in the energy equation is neglected. The equations of the disturbed state are then obtained,

$$\begin{aligned}
 \text{continuity:} & \quad \nabla \cdot \tilde{\mathbf{V}} = 0, \quad (\tilde{\mathbf{V}} = \tilde{u}\mathbf{i} + \tilde{v}\mathbf{j} + \tilde{w}\mathbf{k}), \\
 \text{momentum:} & \quad \frac{d\tilde{\mathbf{V}}}{dt} = -\frac{\nabla\tilde{P}}{\rho_0} + \nu\nabla^2\tilde{\mathbf{V}} - g\frac{\tilde{\rho}}{\rho_0}\mathbf{k}, \\
 \text{energy and diffusion:} & \quad \frac{d\tilde{T}_j}{dt} = K_j\nabla^2\tilde{T}_j + \phi_j(z), \quad j = 1, 2, \\
 \text{state:} & \quad \tilde{\rho} = \rho_0[1 - \alpha_1(\tilde{T}_1 - T_{10}) + \alpha_2(\tilde{T}_2 - T_{20})],
 \end{aligned} \tag{1}$$

where \tilde{T}_1 , \tilde{T}_2 , $\tilde{\mathbf{V}}$, \tilde{P} , $\tilde{\rho}$ are quite general distributions of temperature, salinity, velocity, pressure and density, respectively; $\phi_1(z)$ and $\phi_2(z)$ are heat and mass source terms, x is the coordinate in flow direction and z is in the vertical. It is assumed that the disturbed state can be described by small perturbations superimposed on the initial variables:

$$\begin{aligned}
 \tilde{u} &= \hat{u}(z) + u, & \tilde{v} &= v, & \tilde{w} &= w, & \tilde{T}_j &= \hat{T}_j(z) + T_j, \\
 \tilde{P} &= \hat{P} + P, & \tilde{\rho} &= \hat{\rho} + \rho, & & & j &= 1, 2.
 \end{aligned} \tag{2}$$

The relations in Eq. (2) are substituted into Eq. (1); the terms satisfying the equations of the undisturbed state cancel identically, and linearization of the resulting equations yields, then,

$$\begin{aligned} \nabla \cdot \mathbf{V} &= 0, \quad (\mathbf{V} = ui + vj + wk), \\ \frac{\partial \mathbf{V}}{\partial t} + \dot{u} \frac{\partial \mathbf{V}}{\partial x} + w \frac{d\dot{u}}{dz} \mathbf{i} &= \nu \nabla^2 \mathbf{V} - \frac{\nabla P}{\rho_0} - g(-\alpha_1 T_1 + \alpha_2 T_2) \mathbf{k}, \\ \frac{\partial T_j}{\partial t} + \dot{u} \frac{\partial T_j}{\partial x} + w \frac{dT_j}{dz} &= K_j \nabla^2 T_j, \quad j = 1, 2. \end{aligned} \quad (3)$$

The initial disturbances can be expanded into normal modes, and a solution of Eq. (3) is sought in the form:

$$\begin{aligned} \{ \mathbf{V}(x, y, z, t); T_j(x, y, z, t); P(x, y, z, t) \} \\ = \{ \mathbf{V}(z); T_j(z); P(z) \} \exp[i(\beta_x x + \beta_y y) + \sigma t], \quad j = 1, 2, \end{aligned} \quad (4)$$

where β_x, β_y are the wave numbers and σ is the stability parameter. The three-dimensional perturbation system (4), including waves in the horizontal x, y plane, has been chosen for the case of unbounded flow in these directions (or a flow far from vertical partitions). Substitution of Eq. (4) into Eq. (3) yields:

$$\begin{aligned} (\sigma + i\beta_x \dot{u}) T_j + D \dot{T}_j w &= K_j (D^2 - \beta^2) T_j, \quad j = 1, 2, \\ (\sigma + i\beta_x \dot{u}) \mathbf{V} + D \dot{u} w \mathbf{i} &= \nu (D^2 - \beta^2) \mathbf{V} - \frac{1}{\rho_0} [i(\beta_x \mathbf{i} + \beta_y \mathbf{j}) + kD] P \\ &\quad + g(\alpha_1 T_1 - \alpha_2 T_2) \mathbf{k}, \\ i(\beta_x u + \beta_y v) + Dw &= 0 \end{aligned} \quad (5)$$

where $D = d/dz$ and $\beta^2 = \beta_x^2 + \beta_y^2$. Scalar multiplication of the vector differential operator $D' \equiv i(\beta_x \mathbf{i} + \beta_y \mathbf{j})D + \beta^2 \mathbf{k}$ and the second equation of (5) yields, together with the last of Eqs. (5),

$$\begin{aligned} [K_j (D^2 - \beta^2) - i\beta_x \dot{u}] T_j - D \dot{T}_j w &= \sigma T_j, \quad j = 1, 2, \\ -\{ \nu (D^2 - \beta^2)^2 - i\beta_x [\dot{u} (D^2 - \beta^2) - D^2 \dot{u}] \} w &+ \beta^2 g(\alpha_1 T_1 - \alpha_2 T_2) \\ &= -\sigma (D^2 - \beta^2) w. \end{aligned} \quad (6)$$

The boundary conditions can be of various types, e.g. [2],

$$\begin{aligned} w = 0, \quad D^2 w = 0: &\quad \text{free boundary,} \\ w = 0, \quad Dw = 0: &\quad \text{solid boundary,} \\ DT_j + h_2 T_j = 0: &\quad \text{upper boundary,} \quad j = 1, 2, \\ -DT_j + h_1 T_j = 0: &\quad \text{lower boundary,} \quad j = 1, 2. \end{aligned} \quad (7)$$

It is noted that $h = \infty$ for given temperature or salinity on the boundary, and $h = 0$ for given heat or diffusion fluxes.

Let the variables be normalized, using the following scaling relationships:

$$Q = \int_0^d \dot{u}(z) dz, \quad \bar{z} = z/d, \quad \bar{D} = Dd, \quad \bar{\beta} = \beta d, \quad \bar{u} = \dot{u}d/Q,$$

$$\Delta T_j = \dot{T}_j(0) - \dot{T}_j(d), \quad \bar{T}_j = K_j T_j / \Delta T_j Q, \quad \overline{D\dot{T}_j} = -\frac{d}{\Delta T_j} D T_j, \quad (8)$$

$$\bar{w} = wd/Q, \quad \bar{\sigma} = \sigma d^2/\nu, \quad \bar{h}_{ij} = dh_{ij}, \quad i, j = 1, 2,$$

and define also the nondimensional physical parameters:

$$\text{Re} = Q/\nu, \quad P_j = \nu/K_j, \quad S_j = \frac{g\Delta T_j \alpha_j d^3}{\nu K_j}, \quad R = \beta_x \text{Re}, \quad j = 1, 2, \quad (9)$$

where Re is the Reynolds number, P_j are the Prandtl numbers for temperature and salinity (the latter is also known as the Schmidt number) and $S_j \equiv \text{Ra}_j$ are the corresponding Rayleigh numbers. Introduction of Eq. (8) into Eqs. (6) and (7) reduces these to the dimensionless form

$$(D^2 - \beta^2 - iRP_j\dot{u})T_j + D\dot{T}_j w = \sigma P_j T_j, \quad j = 1, 2,$$

$$- \left\{ (D^2 - \beta^2)^2 - iR[\dot{u}(D^2 - \beta^2) - D^2\dot{u}] \right\} w + \beta^2(S_1 T_1 - S_2 T_2)$$

$$= -\sigma(D^2 - \beta^2)w, \quad (10)$$

and the form of the boundary conditions (7) remains unchanged.

Equations (10) and (7) constitute the mathematical definition of the stability problem; it is an eigenvalue problem, set by three ordinary differential equations with complex coefficients. In general, this problem is not self-adjoint and the stability parameter σ cannot be assumed real. The stability criterion is

$$\text{Real}(\sigma) \leq 0. \quad (11)$$

For given $\dot{u}(z)$, $\dot{T}_1(z)$, $\dot{T}_2(z)$ the flow is stable when the combination of the physical parameters of the problem $\{h_{ij}, P_j, S_j, \text{Re}\}$ guarantees that condition (11) is satisfied for every possible mode (i.e., for every wave number in the range $0 \leq \beta < \infty$, $0 \leq \beta_x \leq \beta$).

3. The stability chart

3.1. General properties

For a complete stability study of a two-dimensional flow, one must analyze general *three-dimensional* disturbances, see Eqs. (4). It is noted that Eqs. (10) depend on both the

physical parameters S_j , P_j , h_{ij} , Re and on the wave numbers in the horizontal and in the flow directions, β and β_x . These determine the modes of the transient perturbations: transverse two-dimensional rolls in the flow direction when $\beta = \beta_x$ and longitudinal two-dimensional rolls perpendicular to it when $\beta = \beta_y \neq 0$, $\beta_x = 0$, or three-dimensional waves at any other angle. A flow is stable if and only if all possible perturbations decay with time; it is therefore necessary to investigate the whole range $0 \leq \beta < \infty$, $0 \leq \beta_x \leq \beta$.

The stability chart in the plane of the temperature and salinity Rayleigh numbers (S_1 , S_2) is obtained from the condition (11) for specific values of P_1 , P_2 and h_{ij} . Marginal stability curves for a fixed value of the Reynolds number Re can be obtained as a family of lines with β_x and β as parameters. The envelope of these curves with respect to these two parameters is the general stability boundary (still for fixed Re). The numerical construction of such a map is rather lengthy. It is therefore desirable to reduce the number of parameters, β and β_x , if possible, from two to one.

The method outlined in this work includes, as a first stage, the derivation of the stability chart for 2-D * perturbations in the flow direction ($\beta = \beta_x$). In general, on some parts of the marginal stability curves of this chart, these disturbances could be the critical ones ("the easiest to excite"). These parts are henceforth denoted "true parts". As to the other parts of the curves, a complete 3-D analysis shows that there exist critical perturbations with a component not in the flow direction. These parts of the curves are denoted "dummy parts", and do not belong to the true general stability boundary.

The following analysis seeks conditions to discriminate between true and dummy parts. The procedure consists of the construction of a general stability chart for 3-D perturbations by the study and modifications of a chart for 2-D transverse disturbance modes. This is considered to be an extension of the Squire theorem [11], c.f. [6], [9].

3.2. The effect of the Reynolds number

Consider various disturbances with a fixed wave number $\beta = \beta_0$. Each state corresponds to a fixed point in the S_1 , S_2 plane with a specific value of the Reynolds number. The state is represented in Fig. 1 as a circle with radius $\beta_0 Re$. It includes all possible disturbance modes (β_x , $0 \leq \beta_x \leq \beta_0$), three of which are shown as various radius-vectors.

It is noted that while Eqs. (10) include β , the wave number, and the product $R \equiv Re \beta_x$, they do not include separately Re , β_x or β_y . Furthermore, the shapes of the dimensionless distributions \hat{u} , \hat{T}_1 , \hat{T}_2 do not depend at all on the value of the Reynolds number. These observations lead to the proof of the Squire theorem: For every three-dimensional disturbance "p" ($\beta_p = \beta_0$, $\beta_{xp} < \beta_0$, Re_A) to state A there exists an equivalent transverse two-dimensional one to another state, B , with smaller Re , "q" ($\beta_q = \beta_0$, $\beta_{xq} = \beta_0$, $Re_B = Re_A \beta_{xp} / \beta_0$). These two modes have, indeed, the same parameters R and β , and therefore the basic Eqs. (10) are the same for both, and the disturbances "p" and "q" are equivalent (see also Fig. 2).

It is noted that this proof of the Squire theorem is somewhat simpler than earlier proofs, e.g. [9]. In the following we consider these modes "p" and "q", and the corresponding states A and B , where A includes mode "p" and all the other possible modes (other values of β_x), and similarly for state B .

On the basis of the equivalence of "p" and "q", Koppel [6] has suggested to use only the 2-D disturbances for the stability study. However, the fact that two states (A and B)

* For brevity, three- and two-dimensional (perturbations) are denoted by 3-D and 2-D, respectively.

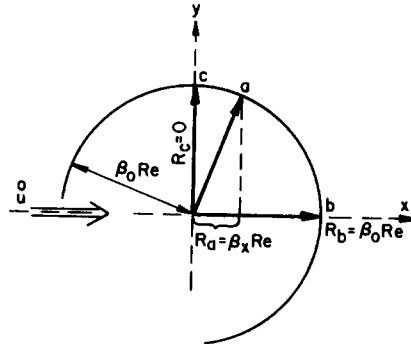


Figure 1. Disturbance patterns to a state with fixed values of the Rayleigh numbers S_1, S_2 and for a specific value of the Reynolds number Re and the wave number, $\beta = \beta_0$. (a) Three-dimensional perturbation. (b) Two-dimensional perturbation in the flow direction. (c) Two-dimensional perturbation perpendicular to the flow direction.

have two equivalent modes (“ p ” and “ q ”) does not necessarily mean that these states will be equivalent too, as will be shown below. Indeed, if disturbance “ q ” is unstable, “ p ” will be unstable too, as well as both states A and B . However, if the state B is stable (for all modes), the disturbance “ q ” will also be stable. Therefore “ p ” is also stable, but state A may still include another unstable mode. Furthermore, when state B is unstable, but disturbance “ q ” is stable, no conclusion can be drawn about the stability of state A . These examples indicate that the use of the Squire theorem requires an additional check in order to determine whether a transverse roll is the most unstable perturbation (see also [9]).

Now, let the shapes of the dimensionless distributions \hat{u}, \hat{T}_j be fixed. The following statements can be made:

I. If a specific point (state) in the S_1, S_2 plane with no flow is unstable, then the introduction of a (horizontal) flow cannot stabilize this point.

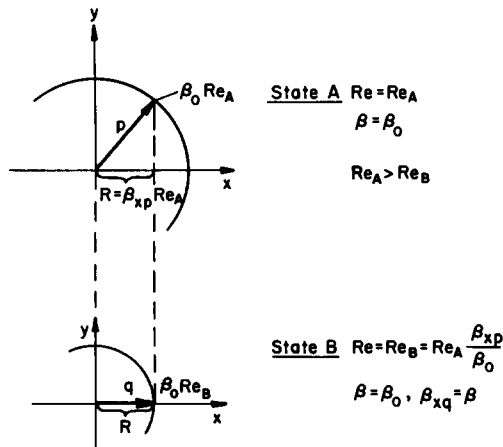


Figure 2. Illustration of the Squire theorem concerning an equivalent 2-D perturbation in the flow direction to a general 3-D perturbation of another state with a larger value of Re .

Proof: Let a certain state \tilde{A} with no flow ($\text{Re} = 0$) be unstable for a certain wave number $\tilde{\beta} = \beta_0$. Suppose that in a new state A^* a flow is formed with a velocity distribution $\tilde{u}(z)$ and a finite Reynolds number, $\text{Re}^* \neq 0$. The state A^* includes a longitudinal disturbance mode ($\beta_y^* = \beta^* = \beta_0$, $\beta_x^* = 0$), which is equivalent to every unstable mode of state \tilde{A} (i.e.: $\tilde{R} = R^* = 0$ and $\beta^* = \tilde{\beta} = \beta_0$). Therefore state A^* is also unstable.

II. If a state \tilde{A} is unstable for $\tilde{\text{Re}}$, $\tilde{\beta}_x$, where $0 < \tilde{\beta}_x < \tilde{\beta} = \beta_0$ (i.e., the unstable disturbance is neither transverse nor longitudinal), then there exists another unstable state $\tilde{\tilde{A}}$ with a lower Reynolds number, $\tilde{\tilde{\text{Re}}} < \tilde{\text{Re}}$. The perturbation destabilizing the state \tilde{A} is in the flow direction with $\tilde{\tilde{\beta}}_x = \tilde{\tilde{\beta}} = \beta_0$, $\tilde{\tilde{\beta}}_y = 0$ and $\tilde{\tilde{\text{Re}}} = \tilde{\beta}_x \tilde{\text{Re}}/\beta_0$.

Proof: The proof immediately follows from the Squire theorem (see above).

III. If a state \tilde{A} is unstable at $\tilde{\text{Re}}$ for a transverse roll, $\tilde{\beta}_x = \tilde{\beta} = \beta_0$, then every other state A^* with a larger Reynolds number, $\text{Re}^* > \tilde{\text{Re}}$, is also unstable.

Proof. Examine for state A^* the disturbance with $\beta^* = \tilde{\beta}$, $\beta_x^* = \tilde{\beta} \tilde{\text{Re}}/\text{Re}^* < \beta^*$. This disturbance is equivalent to the transverse unstable one of state \tilde{A} (i.e.: $R^* = \tilde{R}$, $\beta^* = \tilde{\beta}$), thus A^* is also unstable.

Results:

(a) If the increase of the Reynolds number Re (from zero or a finite value) leads to an instability of an initially stable point in the S_1, S_2 plane, then the first unstable perturbation mode, corresponding to the smallest Re , is transverse.

This result immediately follows from the Squire theorem, e.g. by a consideration of states A and B in Fig. 2, with an additional assumption that the Point S_1, S_2 (corresponding to these states) was stable for some $\text{Re} < \text{Re}_B$.

It follows from statement III above that:

(b) An increase of the Reynolds number cannot stabilize an initially unstable point, or, in other words, it cannot enlarge the stability domain.

Let us suppose, now, that the stability chart has been constructed for 2-D transverse modes ($\beta_x = \beta_0$, $\beta_y = 0$). In order to understand the properties of such a chart and to obtain from it the general stability boundaries (for 3-D disturbances), consider the following additional results:

(c) Suppose that a part of the marginal stability line for a specific value Re^* belongs to the unstable region for $\tilde{\text{Re}}$, where $0 \leq \tilde{\text{Re}} < \text{Re}^*$. This means that there exists an unstable 2-D transverse perturbation with $\tilde{\beta}_x = \beta_0$ and $\text{Re} = \tilde{\text{Re}}$. Thus for every point of this part (corresponding to $\text{Re} = \text{Re}^*$) there exists an unstable 3-D disturbance mode with $\text{Re} = \text{Re}^*$, $\beta = \beta_0$ and $\beta_x^* = \beta_0 \tilde{\text{Re}}/\text{Re}^*$. Therefore, this part is “dummy” by definition.

(d) A similar result is also obtained for a state A which lies inside the stable domain for Re^* . Moreover, if $\text{Re} \neq 0$ and the point A belongs to the statical stability region corresponding to $\text{Re} = 0$, then both the 2-D transverse and longitudinal perturbations are stable for Re^* . However this state (point A with Re^*) will be unstable with respect to a 3-D disturbance (see result c).

It is noted that the statements I–III and the results a–d constitute a complete general

* A support of this hypothesis can be found in [12] as well as in the work of Linden [10], who writes: “there is a significant stabilization of the transverse mode even for very small shears”.

system for describing the influence of the Reynolds number on the stability of double-diffusive flows. Several parts of this system have been formulated earlier for special cases. The derivation and the method of proof presented here are new and general. They are based on the basic eigenvalue equations only, with no restriction to special cases. Two new major results are that the increase of the Reynolds number cannot enlarge the stability domain and that a flow may be unstable with respect to a three-dimensional perturbation even though it is stable for two-dimensional ones in the flow direction and perpendicular to it. Several authors, e.g. Ingersoll [8] and Linden [10], found that for a statically unstable state the most dangerous disturbances are longitudinal rolls. On the other hand, at high Reynolds numbers, transverse rolls are the most unstable modes, c.f. Gage and Reid [9]. Ingersoll [8] and Deardorff [7] considered separately transverse and longitudinal perturbations and determined stability according to the easiest to excite between them. It follows from the result d above that a flow can be unstable, even when these two modes are stable.

The system of statements and results in this section is correct not only for the operators of Eqs. (10), but also for more general problems, provided that the following conditions hold: (a) the undisturbed dimensionless distributions ($\hat{u}(z)$, $\hat{T}_i(z)$ in our case) do not depend on the value of the Reynolds number, (b) the operators of the eigenvalue problem include only the wave number $\beta = (\beta_x^2 + \beta_y^2)^{1/2}$ and the parameter $R \equiv \text{Re } \beta_x$ (and not β_x , β_y and Re separately). An example of such a problem is the stability of flows with thermal diffusion (the Soret effect), treated by Legros and Platten [13].

3.3. Derivation of the stability chart for three-dimensional perturbations

Let us consider first the stability chart for 2-D perturbations in the flow direction ($\beta_x = \beta_0$, $R = \beta_0 \text{Re}$), as shown in Fig. 3. This chart has been obtained in [12], by use of a first-approximation Galerkin method *, for a problem with identical temperature and salinity boundary conditions. The chart includes the following marginal stability lines in the Rayleigh numbers plane (S_1 , S_2) for a fixed value, β_0 , of the wave number, i.e. $\beta_x = \beta = \beta_0$ and for various values of Re :

- (1) ST is the static stability line ($\text{Re} = \text{Re}_0 = 0$);
- (2) ABD, FGH, IJK are the dynamical stability lines for Re_1 , Re_2 and Re_3 respectively; $\text{Re}_3 > \text{Re}_2 > \text{Re}_1 > \text{Re}_0 = 0$. It is shown that the segments BD, GH and JK are true parts while AB, FG and IJ are dummy parts;
- (3) LBGJM is the envelope of the family of the stability lines for various values of Re .

The stability regions in the chart are located to the right and below the corresponding lines for the 2-D disturbances.

Let us consider the infinite triangle F'I'I in Fig. 3. It belongs to the stable domain for Re_3 and to the unstable one for Re_2 , where $\text{Re}_3 > \text{Re}_2$. Therefore, all the points in this region are of the type dealt with in statement d of Section 3.2; they are generally unstable for $\text{Re} = \text{Re}_3$, with respect to a 3-D perturbation mode with $\beta = \beta_0$ and $\beta_x = \beta_0 \text{Re}_2/\text{Re}_3$.

Moreover, the point C lies inside this triangle and also in the statically stable region. Thus for $\text{Re} = \text{Re}_3$ at this point both transverse and longitudinal disturbances are stable, but the state C is generally unstable. Furthermore, consider the line FF'GI'H in Fig. 3,

* This approximation is quite good, as has been demonstrated by a comparison with an exact solution by a general Galerkin method, also obtained by Magen [12].

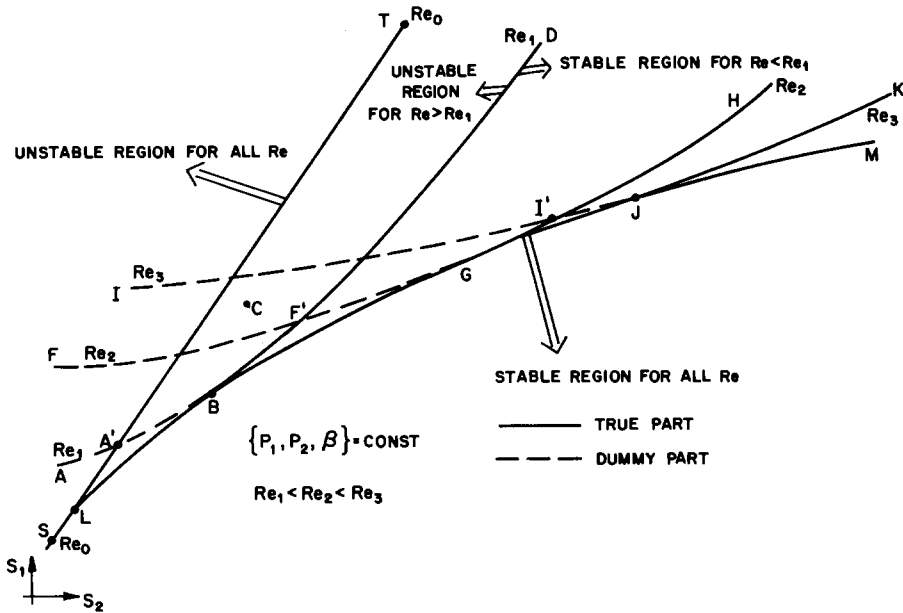


Figure 3. A quantitative scheme of the stability chart in the Rayleigh numbers plane (S_1, S_2).

which is the stability margin for 2-D disturbances, for $Re = Re_2$. The segment FF' belongs to the unstable domain for $Re = Re_1$, where $Re_1 < Re_2$, therefore it is a dummy part, according to statement c. Similarly, the segments AA' and II' are also dummy parts.

Figure 4 illustrates five different states (a–e) with different values of Re corresponding to the point F' in Fig. 3 (the intersection point of the two 2-D boundary lines for Re_1 and Re_2). It can be seen that only the state with $Re = Re_1$ (Fig. 4b) belongs to the true part, while the state with $Re = Re_2$ (Fig. 4d) includes a 2-D marginally stable mode, q , as well as other purely unstable modes. Thus for $Re = Re_2$ the point F' must be considered as unstable and it belongs to the dummy part.

We proceed now to derive the general stability chart for 3-D perturbations from the 2-D one, using the distinction between the true and dummy parts of the marginal stability lines. It is noted, first, that these curves consist of a family of crossing lines with Re as a parameter. It can be seen from Fig. 3 that the envelope of this family, $LBGJM$, divides any marginal stability line such that the segment to the right of the point where both are tangent is a true part. The segment to the left of this point, extending into the unstable domain, is a dummy part. For example, the part JK of the line IJK for $Re = Re_3$ is “true” while the part IJ is “dummy”, where the envelope touches this line at the point J . We recall that a true part is a stability boundary, where a 2-D transverse perturbation is the most dangerous one and therefore it belongs to the general stability chart. On the other hand, the dummy parts must be excluded from the chart, because they correspond to states which are unstable with respect to 3-D modes. Therefore the general marginal stability line for a specific value of the Reynolds number Re and for any perturbation (in any direction) with a wave number β_0 , consists of three parts:

- (1) A true part of the marginal stability line for this Re (in which a 2-D transverse perturbation is, indeed, the most unstable), e.g. the segment HG for $Re = Re_2$ in Fig. 3.

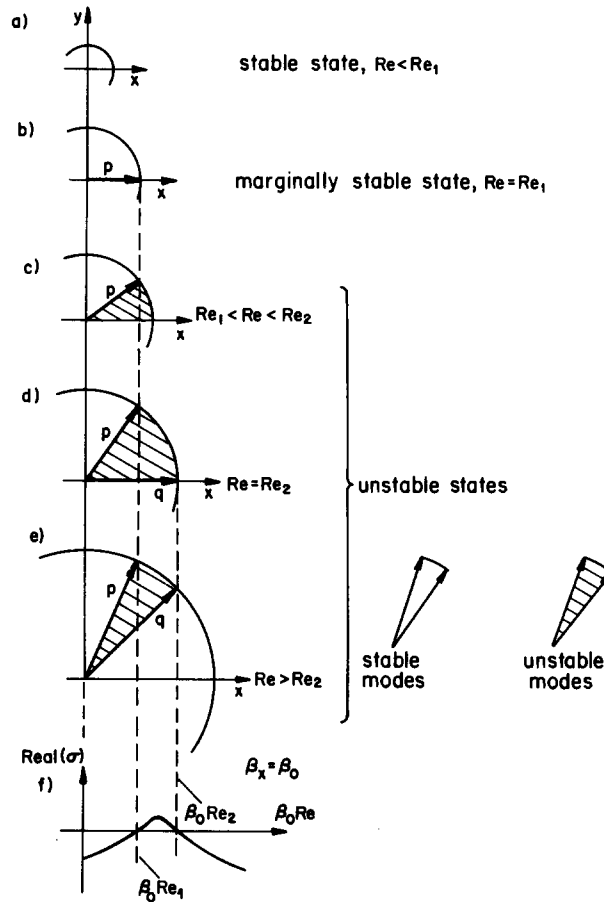


Figure 4. Illustration of stable and unstable states (a–e) for the point F' in Fig. 3. p and q are marginally stable modes. The bottom curve (f) represents the real part of the largest eigenvalue, $\text{Real}(\sigma)$, as a function of $\beta_0 \text{Re}$, when only 2-D disturbances are considered.

- (2) The part of the envelope to the family of lines for various Re , starting from the point where it is tangent to the previous line, up to the point where it is tangent to the stactical stability line (for $\text{Re} = 0$), e.g. the segment GL in Fig. 3.
- (3) A part of the stactical stability line, e.g. LS in Fig. 3. This follows from the result that the stability domain cannot increase as a result of an increase of Re .

The Rayleigh numbers plane (S_1, S_2) can be divided into four different stability regions, for a given value of the Reynolds number Re_1 (see Fig. 3):

- (1) General or stactical instability (left of the line ST), where every point is unstable for all values of Re , including $\text{Re} = 0$.
- (2) Instability, where every point is unstable for $\text{Re} > \text{Re}_1$ (the region $TLBD$ for $\text{Re} = \text{Re}_1$).
- (3) Stability where every point is stable for $\text{Re} < \text{Re}_1$ (DBM for $\text{Re} = \text{Re}_1$).
- (4) General stability, where every point is stable for all Re (the region below and right of $SLBGJM$).

Finally, consider a point G on the envelope, with some specified value of the Reynolds number (say Re^*). This point lies on the margin FGH for $Re = Re_2$, so if $Re^* < Re_2$, the point G is stable. If $Re^* = Re_2$, this state (point G with Re_2) includes one marginally stable disturbance in the flow direction ($\beta_x = \beta_0$), and if $Re^* \geq Re_2$, the point G is marginally stable for the 3-D disturbance with $\beta_x = \beta_0 Re_2/Re^*$. In this case both disturbances p and q in Figs. 4d, 4e converge, the unstable region (between p and q) disappears, and the maximum of $Real(\sigma)$ in Fig. 4f toughes the axis $\beta_0 Re$, thus $Real(\sigma) \leq 0$.

3.4. Conditions for the true parts of marginal stability lines

In the previous section the division between true and dummy parts of the marginal stability lines has been illustrated as the geometrical construction of the envelope to the family of lines for various Re . More rigorous conditions for the division are derived in this section, in order to avoid the lengthy (and expensive) numerical calculations involved in the construction of the full 2-D stability chart and the required envelope.

Consider a point on a true part of a marginal stability line, say H for $Re = Re_2$ in Fig. 3. When the Reynolds number is increased, say to Re_3 , the stability margin moves into the stability domain, e.g. to the line JK and the point H is now in the unstable region. This follows from the result that the stability domain cannot increase upon an increase in Re . Therefore, the condition $\partial[Real(\sigma)]/\partial Re > 0$ must hold at every point of any true part. By the same argument it can be shown that the condition $\partial[Real(\sigma)]/\partial Re < 0$ holds at every point on any dummy part. σ here is the eigenvalue with the largest real part, corresponding to the marginal stability perturbation at the point considered, ($Real(\sigma) = 0$). In addition it can be shown that on the envelope (LBGJM) the inequality reduces to an equality, i.e.:

$$Real(\sigma) = 0, \quad \frac{\partial[Real(\sigma)]}{\partial Re} \begin{cases} > 0, & \text{true parts} \\ = 0, & \text{envelope} \\ < 0, & \text{dummy parts} \end{cases} \quad (12)$$

see also Fig. 4f. The conditions (12) have been derived in terms of Re . It is reminded that we study here the general effects of the Reynolds number Re on the stability chart for a specific value of the wave number, $\beta = \beta_0$, e.g. Fig. 3. A further investigation to find the most dangerous disturbance with respect to β would require a numerical solution of the governing equations. This has been done by Magen [12].

To derive analytical expressions from the conditions (12), let us consider the following general eigenvalue problem:

$$L(\xi)x = \sigma M(\xi)x \quad (13)$$

where σ is the eigenvalue (a complex number, in general), x is the eigenelement, belonging to a Hilbert space, H , and L and M are linear operators in H . L and M depend on the parameter ξ . The derivative of σ with respect to ξ , $\dot{\sigma}$, can be obtained when the derivatives of L and M exist (\dot{L} and \dot{M}), and if σ is a simple eigenvalue, c.f. [14,12],

$$\langle x^* \cdot Mx \rangle \dot{\sigma} = \langle x^* \cdot (\dot{L} - \sigma \dot{M})x \rangle \quad (14)$$

where x^* is the eigen-element of the adjoint problem. The notation $\langle u \cdot v \rangle$ represents a scalar product of the elements $u \in H$, $v \in H$ in the space H .

Using Eqs. (10) and (14), the following expression is obtained for the derivative of σ :

$$\begin{aligned} \frac{\partial \sigma}{\partial \text{Re}} = & -i\beta \int_0^1 \{ \dot{u}(\xi) [P_1 \bar{T}_1^*(\xi) T_1(\xi) + P_2 \bar{T}_2^*(\xi) T_2(\xi) \\ & + \bar{w}^*(\xi) (\beta^2 - D^2) w(\xi)] + D^2 \dot{u} \bar{w}^*(\xi) w(\xi) \} d\xi \\ & / \int_0^1 [P_1 \bar{T}_1^*(\xi) T_1(\xi) + P_2 \bar{T}_2^*(\xi) T_2(\xi) + \bar{w}^*(\xi) (\beta^2 - D^2) w(\xi)] d\xi \quad (15) \end{aligned}$$

where $w(\xi)$ and $T_j(\xi)$ are the eigenfunctions of the problem defined by Eqs. (10) and (7) and $w^*(\xi)$ and $T_j^*(\xi)$ are those of the adjoint problem.

It is noted that the solutions for the eigenfunctions are not always required, and in general their derivation is quite complicated. In cases where these are unknown, the condition (12) can be checked as follows: suppose a point in a 2-D marginal stability line has been found for some Re . At this point $\text{Real}(\sigma) = 0$, where σ is the eigenvalue with the largest real part. Re is then slightly increased and this eigenvalue is calculated again. If the result is $d[\text{Real}(\sigma)] < 0$ the point belongs to a dummy part, while if $d[\text{Real}(\sigma)] > 0$ it belongs to a true part.

4. Conclusions

The general properties of the stability chart of double-diffusive processes have been discussed using the structure of the governing equations but not their solutions. The two main results obtained here are: (1) An increase in the Reynolds number cannot increase the stability domain, (2). There may exist flows which are stable for both two-dimensional transverse and longitudinal perturbations, but unstable with respect to a three-dimensional perturbation in a different direction.

The marginal stability lines for various values of Re in the stability chart for 2-D transverse disturbances have been divided into "true" and "dummy" parts. The "true" parts include the points for which the 2-D disturbances are the most destabilizing, and therefore the Squire transform may be directly applied.

The distinction between true and dummy parts has been derived geometrically, using the envelope of the lines for various Re (Fig. 3), and analytically by the relations (12). These conditions are general necessary conditions, which are also sufficient to construct a stability map of the form illustrated in Fig. 3.

References

- [1] S. Ostrach, Unstable convection in vertical channels with heating from below, *NACA Report* TN 3548 (1955).
- [2] S. Chandrasekhar, *Hydrodynamic and hydromagnetic stability*, Oxford University Press (1961).
- [3] G. Veronis, Effect of the stabilizing gradient of solute on thermal convection, *J. Fluid Mech.* 34 (1968) 315–336.
- [4] D. Pnueli and S. Iscovici, Sufficient conditions for stability of completely confined fluids, *Israel J. Tech.* 8 (1970) 209–215.

- [5] D. Pnueli and Y. Zvirin, Stability of stratified fluids – a literature survey, *Report TME-295, Mech. Eng., Technion* (1976).
- [6] D. Koppel, On the stability of flow of a thermally stratified fluid under the action of gravity, *J. Math. Phys.* 5 (1964) 963–982.
- [7] J.W. Deardorff, Gravitational instability between horizontal plates with shear, *Phys. Fluids* 8 (1965) 1027–1030.
- [8] A.P. Ingersoll, Thermal convection with shear at high Rayleigh number, *J. Fluid Mech.* 25 (1966) 209–228.
- [9] K.S. Gage and W.H. Reid, The stability of thermally stratified plane Poiseuille flow, *J. Fluid Mech.* 33 (1968) 21–32.
- [10] P.F. Linden, Salt fingers in a steady shear flow, *Geophysical Fluid Dynamics* 6 (1974) 1–27.
- [11] H.B. Squire, On the stability for three-dimensional disturbances of viscous fluid flow between parallel walls, *Proc. Roy. Soc. A.* 142 (1933) 621–628.
- [12] M. Magen, Thermohaline stability with general horizontal flows. *D.Sc. Thesis, Technion, Haifa, Israel* (1983).
- [13] J.C. Legros and J.K. Platten, Two-component Bénard problem with Poiseuille flow, *J. Non-Equilib. Thermodyn.* 2 (1977) 211–232.
- [14] E. Wasserstrom, Numerical solution by the continuation method, *SIAM Review* 15 (1973) 89–119.